

# The Effect of pH on the Soot Elimination Performance of Pt/CeO<sub>2</sub>-TiO<sub>2</sub>-Al<sub>2</sub>O<sub>3</sub>

HE Junjun<sup>1,2</sup>, ZHENG Tingting<sup>1</sup>, XIA Wenzheng<sup>1</sup>, CHANG Shiyong<sup>1</sup>,  
HUAN Yuanfeng<sup>1,3\*</sup>, ZHAO Yunkun<sup>1,2</sup>

(1. Kunming Sino-platinum Metals Catalysts Co. Ltd., Kunming 650106, China; 2. State Key Laboratory of Advanced Technologies for Comprehensive Utilization of Platinum Metals, Kunming Institute of Precious Metals, Kunming 650106, China; 3. Materials Science and Engineering of Kunming University of Science and Technology, Kunming 650118, China)

**Abstract:** A series of catalysts Pt/CeO<sub>2</sub>-TiO<sub>2</sub>-Al<sub>2</sub>O<sub>3</sub> were prepared by impregnation method using the supports which have large surface area. Through changing the pH of Pt loading process, the soot elimination performance under NO atmosphere was also studied carefully. The results showed that the lower pH of Pt loading process, the catalysts possess greater Pt particle size, larger amount of chemisorbed surface active oxygen species (O<sub>2</sub><sup>-</sup>, O<sup>-</sup>) and better activity. Combining the results of in-situ DRIFT and catalytic activity, it is concluded that bidentate nitrates and adsorbed NO<sub>2</sub> are the active intermediate species. Different concentrations of H<sub>2</sub>O and SO<sub>2</sub> resistant test were carried out on the P3 catalyst, it is found that the performance changed little before and after poisoning, which implies that the stability of catalyst is good.

**Key words:** soot oxidation; ceria-titania-alumina; platinum; pH; *in-situ* DRIFTS

**CIJ number:** TG146.3<sup>+</sup>1 **Document code:** A **Article ID:** 1004-0676(2014)S1-0149-09

## pH 值对 Pt/CeO<sub>2</sub>-TiO<sub>2</sub>-Al<sub>2</sub>O<sub>3</sub> 催化剂碳烟消除性能影响

何俊俊<sup>1,2</sup>, 郑婷婷<sup>1</sup>, 夏文正<sup>1</sup>, 常仕英<sup>1</sup>, 桓源峰<sup>1,3\*</sup>, 赵云昆<sup>1,2</sup>

(1. 昆明贵研催化剂有限责任公司 云南省贵金属催化材料工程技术研究中心, 昆明 650106; 2. 昆明贵金属研究所 稀贵金属综合利用新技术国家重点实验室, 昆明 650106; 3. 昆明理工大学 材料科学与工程学院, 昆明 650118)

**摘要:** 以高比表面积三元复合氧化物作为载体制备 Pt/CeO<sub>2</sub>-TiO<sub>2</sub>-Al<sub>2</sub>O<sub>3</sub> 催化剂, 调控贵金属 Pt 负载过程中的 pH, 研究催化剂体系在 NO 气氛下对碳烟的消除能力。结果表明催化剂合成过程中的 pH 值越低, 催化剂中贵金属粒子越大、同时催化剂中化学吸附的表面活性氧物种(O<sub>2</sub><sup>-</sup>, O<sup>-</sup>)的量越多, 催化剂对碳烟的消除能力越强。原位傅立叶红外表征证明双齿硝酸盐和吸附 NO<sub>2</sub> 是反应所需活性中间物种, 优化制备的催化剂 P3 具有优异的抗 H<sub>2</sub>O 及抗 SO<sub>2</sub> 中毒的性能。

**关键词:** 碳烟氧化; 氧化铈-氧化钛-氧化铝; 铂; pH; 原位红外

In the past decades, diesel engines were widely used due to their superior efficiency, durability and reliability. Nitrogen oxides and particulate matter

emission are two important pollutants in the exhaust from diesel engines<sup>[1]</sup>. In recent years, increasing attention has been paid to diesel engine emissions,

Received: 2014-09-22

Foundation item: 863 Project(2013AA065302).

First author: HE Junjun, male, Ph.D, Research direction: Exhaust control and purification. E-mail: hjj1900@tju.edu.cn

\*Corresponding author: HUAN Yuanfeng, male, professor, Research direction: Exhaust control and purification. E-mail: hyf@jpm.com.cn

especially the particulate matter fraction (PM), consisting mostly of carbonaceous soot and a volatile organic fraction of hydrocarbons condensed or adsorbed over the soot, which are highly hazardous due to its potential mutagenic and carcinogenic activity<sup>[2-3]</sup>. In particular, diesel PM smaller than 2.5  $\mu\text{m}$  (PM<sub>2.5</sub>) does not only penetrate deep in the lungs but remains there longer than larger particles. Consequently, the formulation of restrictive legislation in EU regarding these fine particles is being imposed. The use of a catalytic trap performing both filtration and catalytic combustion of soot appears to be a promising solution for soot removal<sup>[4]</sup>.

To develop suitable catalysts capable of promoting soot oxidation by  $\text{NO}_x$  is an efficient way for removal of diesel soot at low temperature and has been exploited in Johnson Matthey's continuously regeneration technology (CRT)<sup>[5]</sup>. This reduction mostly involves  $\text{NO}_2$  molecules by direct reaction with soot to form NO and, to a much less extent,  $\text{N}_2$  and  $\text{N}_2\text{O}$ <sup>[6-7]</sup>. The current commercial catalyst is Pt based catalyst, but the performance of activity and sulfur-resistance should be improved in practical used.

Ceria has been used as oxygen storage material for three-way catalysts and was proven to be an effective component of soot oxidation catalysts<sup>[8]</sup>. The Alumina has been added to  $\text{CeO}_2$  based mixed oxides as promoters for three-way catalysts to produce nanocomposite materials with thermal stability at temperature up to 1100  $^\circ\text{C}$ <sup>[9]</sup>, however, its sulfur-resistance is poor. Matsumoto et al.<sup>[10]</sup> found that the decomposition temperature of sulfates on  $\text{TiO}_2$  support is lower than that on  $\text{Al}_2\text{O}_3$  support under reducing conditions. Our results show the  $\text{CeO}_2$ - $\text{TiO}_2$ - $\text{Al}_2\text{O}_3$  supported Pt catalyst has better thermal and sulfur resistant performance than single or binary oxides supported catalyst. As far as we know, little work has been performed on Pt/ $\text{CeO}_2$ - $\text{TiO}_2$ - $\text{Al}_2\text{O}_3$  catalysts.

In the present work, the Pt based catalysts were prepared supported by  $\text{CeO}_2$ - $\text{TiO}_2$ - $\text{Al}_2\text{O}_3$  composite oxides. Thus, various physical and spectroscopic characterizations such as  $\text{O}_2$ -TPD, XPS, *In-situ* DRIFTS were performed to investigate the influence of the pH value of Pt loading process on Pt particle

size, surface coverage of Pt, and  $\text{NO}_x$  utilization for NO assisted soot oxidation. The Pt dispersion, active oxygen species and catalytic performance of the catalysts are well correlated. The  $\text{NO}_x$  storage mechanisms and  $\text{H}_2\text{O}$  and  $\text{SO}_2$  resistant performance over these catalysts are also revealed.

## 1 Experimental

### 1.1 Catalyst preparation

$\text{CeO}_2$ - $\text{TiO}_2$ - $\text{Al}_2\text{O}_3$  composite oxides with  $\text{Al}_2\text{O}_3$ ,  $\text{TiO}_2$ ,  $\text{CeO}_2$  content (mass fraction) 54%, 10%, 36% respectively were synthesized by fractional precipitation. First, quantitatively ammonia solution and aluminum solution were slowly added to the beaker simultaneously to prepare aluminium hydroxide under strong stirring, the pH value of the co-precipitating solution was maintained at 8. After stirring 2 h at room temperature, another quantitatively ammonia solution and the solution contain ceria and titanium were added to the aluminium hydroxide simultaneously, the pH was maintained at 8. The obtained precipitate was filtered and thoroughly washed using distilled water, and finally dried at 120  $^\circ\text{C}$ , then the powders were calcined at 650  $^\circ\text{C}$  for 4 h in air atmosphere.

The supported Pt catalysts were prepared by conventional wet impregnation method with an aqueous of  $\text{Pt}(\text{NO}_3)_2$  as metal precursor. The pH of the impregnated samples was adjusted by acetic acid to 3, 4, 5, 6 and to 9 by KOH, the reference sample was not adjusted by any another reagent. After stirring for 2 h, the samples were washed with distilled water until pH=7. After drying at 120  $^\circ\text{C}$  and calcinations at 550  $^\circ\text{C}$  for 4 h, the Pt/ $\text{CeO}_2$ - $\text{TiO}_2$ - $\text{Al}_2\text{O}_3$  samples were obtained, namely Px, x stands for the pH value of Pt loading process.

### 1.2 Characterization technique

The measurement of the specific surface area (SSA) was carried out at -196  $^\circ\text{C}$  on Quantachrome QuadraSorb SI instrument by using the nitrogen adsorption method. The samples were pretreated in vacuum at 300  $^\circ\text{C}$  for 8 h before experiments. The surface area (SSA) was determined by BET method in 0~0.3 partial pressure range.

X-ray diffraction measurement was carried out on an X'pert Pro rotatory diffractometer (PANalytical Company) operating at 40 mA and 40 kV using Co K $\alpha$  as radiation source ( $\lambda=0.1790$  nm). The data of  $2\theta$  from  $20^\circ$  to  $100^\circ$  were collected with a step size of  $0.033^\circ$ .

O<sub>2</sub> temperature-programmed desorption (O<sub>2</sub>-TPD) measurements were conducted on a CHEMBET 3000 apparatus supplied by Quantachrome Company. During the test, 100 mg of each sample were pre-heated in pure O<sub>2</sub> from room temperature to  $500^\circ\text{C}$  and held for 30 min. After cooling to room temperature, the sample was heated from room temperature to  $900^\circ\text{C}$  at a heating rate of  $10^\circ\text{C}/\text{min}$  in pure helium.

X-ray photoelectron spectra (XPS) were recorded with a PHI-1600 ESCA spectrometer using Mg K $\alpha$  radiation (1253.6 eV). The base pressure was  $5\times 10^{-8}$  Pa. The binding energies were calibrated using C1s peak of contaminant carbon (B.E.=284.6 eV) as standard, and quoted with a precision of  $\pm 0.2$  eV. Gaussian-Lorentzian and Shirley background was applied for peak analysis.

In situ DRIFTS experiments were performed on a Nicolet Nexus FT-IR spectrometer, equipped with a MCT detector and a heating chamber allowing samples to be heated up to  $600^\circ\text{C}$ . The DRIFT spectra were recorded against a background spectrum of the sample purified just prior to introducing the adsorbates. Each time, about 15 mg of the sample was used. The sample was firstly pretreated under (volume fraction) 5% O<sub>2</sub>/He at  $100^\circ\text{C}$  for 30 min, and then exposed to a flow of  $400\times 10^{-6}$  NO+10% O<sub>2</sub> + balance He. The spectra of NO<sub>x</sub> adsorption from  $200$  to  $500^\circ\text{C}$  at intervals of  $50^\circ\text{C}$  were recorded with a resolution of  $4\text{ cm}^{-1}$ .

### 1.3 Pretreatment method with sulfur and water

Light diesel engine exhaust is a multi-component system, especially contains water and sulfur, so the catalyst samples were pretreated in the atmosphere containing water and sulfur to reflect the catalyst performance in the real situation. The pretreatment atmospheres included (a) 5% H<sub>2</sub>O + N<sub>2</sub>; (b) 10% H<sub>2</sub>O + N<sub>2</sub>; (c)  $50\times 10^{-6}$  SO<sub>2</sub>, 10% O<sub>2</sub>, N<sub>2</sub> as balance; (d)

$250\times 10^{-6}$  SO<sub>2</sub>, 10% O<sub>2</sub>, N<sub>2</sub> as balance. The total flow rate was 120 mL/min. Before test, 0.3 g sample were pretreated at the above four mentioned atmospheres for 2 h with the temperature of micro reactor was set to  $350^\circ\text{C}$ . After pretreatment, the samples were dried at  $150^\circ\text{C}$ , and used for TG/DTA test.

### 1.4 Activity measurement

For soot combustion, the catalytic activity of the prepared samples was evaluated by TG/DTA technique using Degussa Printex-U as the model soot, which possesses a specific surface area of  $100\text{ m}^2/\text{g}$  and an average particle size of  $25\pm 3$  nm (C: 92.2%; H: 0.6%; volatiles: 6%, in mass fraction)<sup>[11]</sup>, its morphology could be seen in Fig.1<sup>[12]</sup>. The soot was mixed with the catalyst to obtain a tight contact in a weight ratio of 1:20. Then, the mixture (8 mg) was loaded to the sample chamber and heated from room temperature to  $800^\circ\text{C}$  at a rate of  $10^\circ\text{C}/\text{min}$  in the atmosphere of (volume fraction)  $400\times 10^{-6}$  NO and 10% O<sub>2</sub> balanced by N<sub>2</sub>. By comparing characteristic temperatures of TG/DTA profiles, the catalytic activity of the samples was determined. In this work, the temperatures corresponding to soot ignition (denoted as  $T_i$ ), maximal soot combustion rate (denoted as  $T_m$ ) and the complete soot conversion (denoted as  $T_c$ ) were used to evaluate the performance of the catalysts.

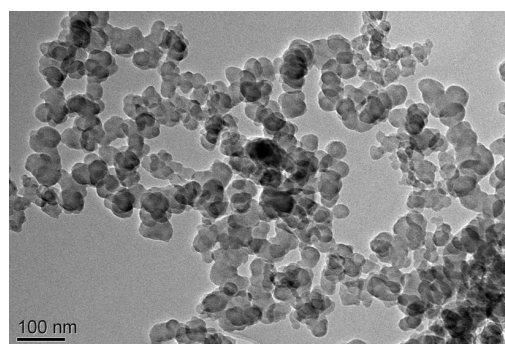


Fig.1 TEM images of soot particles (Printex-U)

图 1 碳烟颗粒的 TEM 图

## 2 Results and discussion

### 2.1 N<sub>2</sub> adsorption-desorption measurement

The N<sub>2</sub> adsorption/desorption isotherms and pore size distribution from desorption branch of the

isotherm by BJH method for different catalyst samples are shown in Fig.2. The comparison of isotherms reported in Fig.2 shows the catalyst P3, P7 and P9 have the similar adsorption/desorption isotherms, and the isotherms of all the samples exhibit a typical reversible type IV curve (IUPAC classification) with hysteresis loops<sup>[13]</sup>, it means that the inflection point corresponding  $p/p_0$  belongs to the range of mesoporous. The result of pore size distribution shows that the sample is relatively uniform. As it can be seen in Tab.1, P3, P7 and P9 show almost the same BET

surface area, cumulative pore volume and pore diameter. Compared with the pure support (202.5  $m^2/g$ ), after loading Pt, the surface area of support increased a little because of the increase of surface hole which caused by acid “corrosion”. The pH adjust in the Pt loading process has no influence on the catalyst surface area, pore volume and pore diameter. This shows that the change of the catalyst activity should be attributed to other factors, such as precious metal dispersion, activated oxygen ability of catalyst etc.

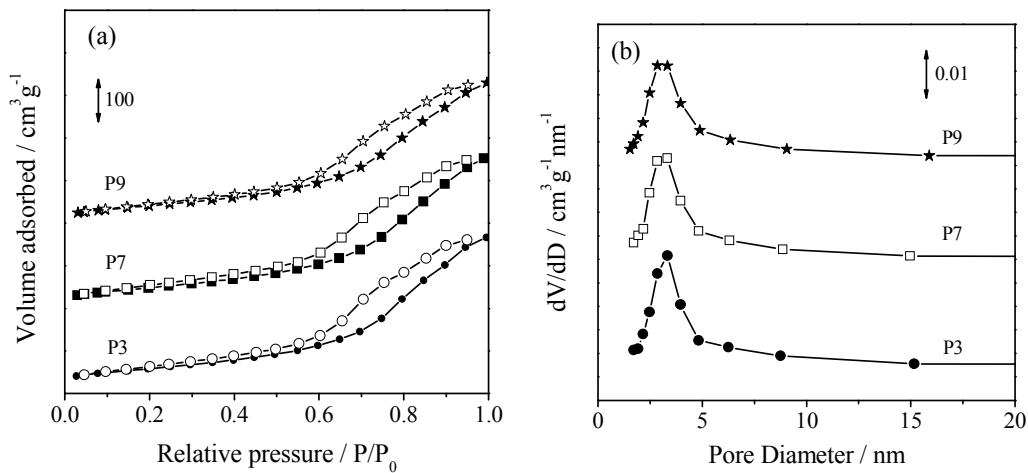


Fig.2 N<sub>2</sub> adsorption/desorption isotherms (a) and pore size distribution (b)

图 2 N<sub>2</sub> 吸附/脱附曲线(a)和孔径分布图(b)

Tab.1 S<sub>BET</sub>, D<sub>Pt</sub> and T<sub>i</sub>, T<sub>m</sub>, T<sub>f</sub> of different samples

表 1 不同样品的比表面积, Pt 分散度和转化温度 T<sub>i</sub>, T<sub>m</sub>, T<sub>f</sub>

Catalysts	Activity/°C			S <sub>BET</sub> / (m <sup>2</sup> /g)	H/Pt	D <sub>Pt</sub> from H/Pt <sup>[14]</sup> /nm
	T <sub>i</sub>	T <sub>m</sub>	T <sub>f</sub>			
P3	235	370	465	210.2	0.31	3.7
P4	253	382	467	—	—	—
P5	265	402	480	—	0.35	3.2
P6	273	420	490	—	—	—
P7	280	420	505	212.9	0.47	2.4
P9	300	440	528	215.6	0.52	2.2

2.2 Catalytic activity for soot combustion

The soot elimination activity was tested on the TG/DTA under NO auxiliary atmosphere, the results are shown in Tab.1 and Fig.3. The characteristic temperature T<sub>i</sub>, T<sub>m</sub> and T<sub>f</sub> were used to indicate the soot oxidation activity in NO atmosphere.

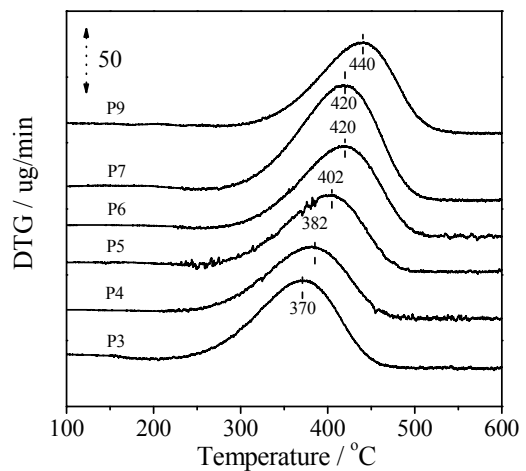


Fig.3 DTG curves for different catalysts (the reaction atmosphere was  $400 \times 10^{-6}$  NO + 10% O<sub>2</sub> + N<sub>2</sub>)

图 3 不同催化剂的 DTG 曲线(反应气氛  $400 \times 10^{-6}$  NO + 10% O<sub>2</sub> + N<sub>2</sub>)

From the test results in Fig.3, it can be seen that the  $T_m$  of P7 is 420 °C, with the decrease of pH, the  $T_m$  is decreased significantly, then the soot combustion activity is improved, and it works the other way as well. P3 has the best activity, the  $T_m$  is only 370 °C,

compared with P7, the  $T_m$  is reduced by 50 °C.

### 2.3 Results of H<sub>2</sub>-pulsing and HRTEM

H<sub>2</sub>-pulsing and HRTEM were used to investigate the particle size of precious metal in the catalysts, the results are shown in Tab.1 and Fig.4.

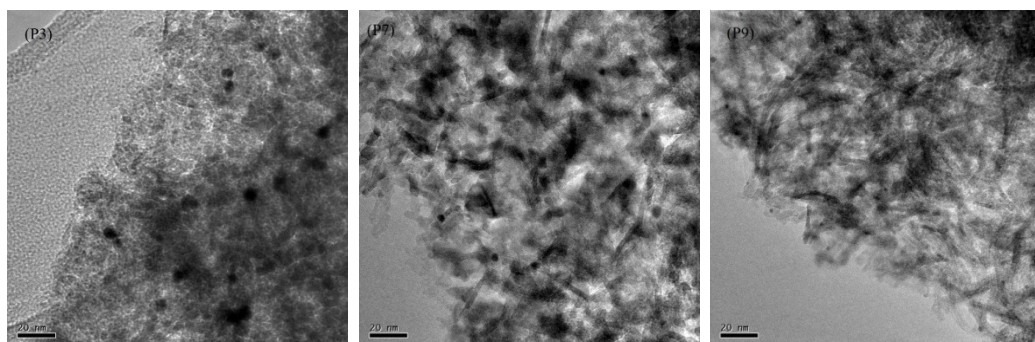


Fig.4 HRTEM images of the catalysts: (Left) P3; (Middle) P7; (Right) P9

图 4 催化剂的高分辨透射电镜图: (左) P3; (中) P7; (右) P9

As seen from Tab.1, with the reduction of pH value in the process of catalyst synthesis, Pt particle size in catalyst gradually increased, it is demonstrated that different thermodynamic behaviors in the process of synthesis affect the particle size of Pt (as shown in Fig.5): HAc emits a large amount of heat in the process of decomposition, moreover precious metals

have a promoting effect on the organic matter decomposition, this kind of phenomenon will lead to local high temperature near the Pt precursor which is adjacent to acetic acid, and then causes precious metals sintering and particle growth. Similar phenomenon was also confirmed by other research institute<sup>[15-16]</sup>.

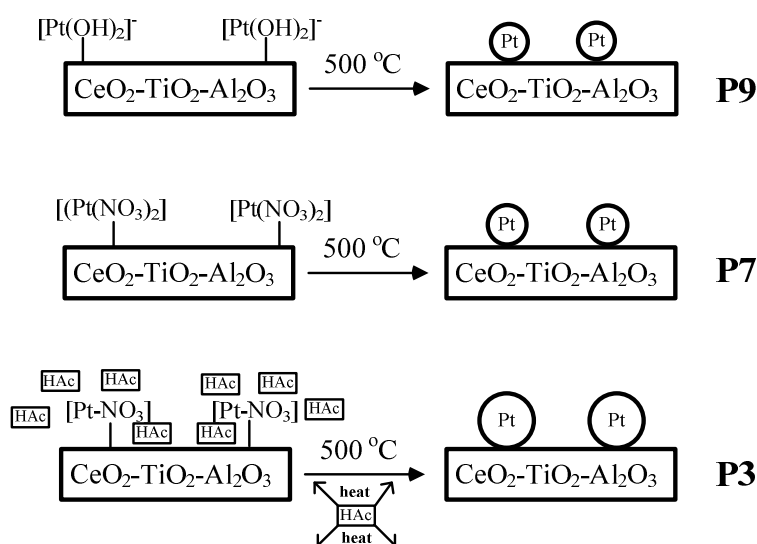


Fig. 5 The scheme of Pt particles growth during calcinations

图 5 老化过程中 Pt 粒子的团聚示意图

HRTEM was used to observe the size and morphology of Pt particles, on the different samples. From Fig.4 it can be concluded that Pt particles are less than

5 nm in all samples. The lower the pH value in the process of catalyst synthesis, the larger Pt particles are, this is consistent with the H<sub>2</sub> pulsing results. In

addition,  $\text{Al}_2\text{O}_3$  exists in the form of amorphous and crystalline states from the TEM result. A large number of research reports confirmed that Pt oxidation NO into  $\text{NO}_2$  is a structure sensitive reaction<sup>[17-18]</sup>, and the NO oxidation reaction activity with Pt is the strongest when the Pt particle size is around 4 nm, this is because the  $\text{NO}_2$  oxidizability is much stronger than  $\text{O}_2$  and NO, and in the soot elimination reaction with  $\text{NO}+\text{O}_2$  atmosphere, whether  $\text{NO}_2$  is easy to produce and the production has an important impact on activity. According to some conclusions, the larger the Pt particle size is, the more the  $\text{NO}_2$  species produced in the reaction are, then it is conducive to the soot elimination (The phenomenon is consistent with the situ infrared results). Furthermore, some studies reported that the larger Pt particles in the catalyst, the better the elimination activity for intermediate species that were generated in the soot oxidation process<sup>[19-20]</sup>. In brief, the greater the Pt particle size is in a certain range, the better the activity of catalyst<sup>[21]</sup>.

## 2.4 Results of $\text{O}_2$ -TPD

$\text{O}_2$ -TPD was used to study the oxygen activation and adsorption on the Pt catalyst, as show in Fig.6.

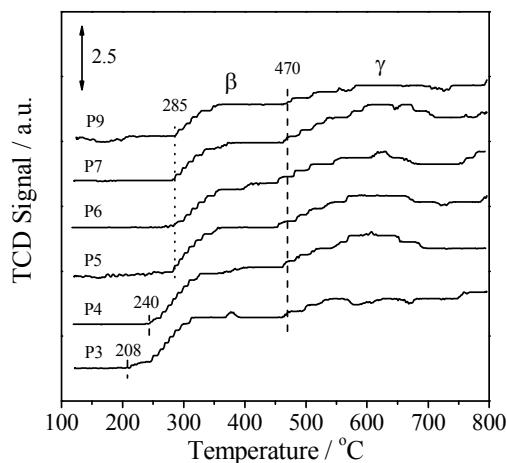


Fig.6  $\text{O}_2$ -TPD curves of Pt/ $\text{CeO}_2$ - $\text{TiO}_2$ - $\text{Al}_2\text{O}_3$  catalysts

图 6 Pt/ $\text{CeO}_2$ - $\text{TiO}_2$ - $\text{Al}_2\text{O}_3$  催化剂的  $\text{O}_2$ -TPD 图

The pH adjustment in the Pt loading directly affects the oxygen activity and adsorption of the catalyst. The start desorption temperatures of P5~P9 are close to each other, about 285 °C, but the desorption temperature of P4 is reduced to 240°C, P3 is the lowest, about 208 °C. The desorption peak

between 200~470 °C can be attributed to the chemical surface activity oxygen species ( $\text{O}_2^-$ ,  $\text{O}^-$ ), the higher temperature desorption peak is the lattice oxygen ( $\text{O}^{2-}$ )<sup>[22]</sup>. Although, it is difficult to semi-quantitatively analyze the amount of surface active oxygen species, but it is also visualized found that the amount of surface active oxygen species of Py ( $y=3, 4, 5, 6$ ) samples gradually increase with the pH decreased compared with P7 sample, especially the  $\beta$  active oxygen species. In addition, with the increase of pH, P9 sample has the opposite regular than the P7 sample. According to the above analysis, Pt has a strong metal-support interaction with  $\text{CeO}_2$ - $\text{TiO}_2$ - $\text{Al}_2\text{O}_3$ , and the pH in the preparation is the key factor that affects the strong interaction. So it is deduced that the charge distribution between small Pt cluster and support can weaken the Ce(Ti)-O bond and improve the mobility of reactive oxygen species.

## 2.5 Result of XPS

The XPS spectra of all catalysts are shown in Fig.7.

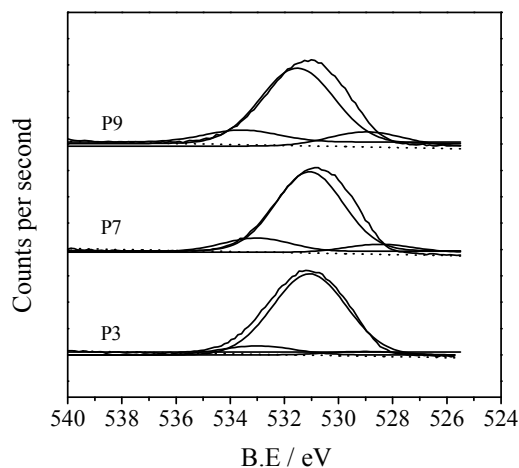


Fig.7  $\text{O}1s$  XPS spectra of catalysts (P3, P7, P9)

图 7 催化剂的  $\text{O}1s$  XPS 谱图(P3、P7、P9)

The oxygen species of all samples mainly have three chemical states, the binding energy of  $\alpha$  oxygen species is between 528.0 and 528.2 eV, in 530.5 and 531.1 eV is  $\beta$  oxygen species, and the binding energy of the  $\gamma$  oxygen species lies between 531.8 and 532.4 eV, this three could be belong to lattice oxygen  $\text{O}^{2-}$ ,  $\text{O}^-$  species and  $\text{O}_2^-$ <sup>[23-24]</sup>. As seen from figure, with the decrease of pH value, the binding energy of  $\text{O}1s$

shifting from the high binding energy direction, it suggested that the surface adsorption oxygen species are increased. As the O1s XPS spectrum peak of sample is asymmetry, thus the standard Gaussian-Lorentz method was used to fitting analysis, according to the different proportions of integral area, the relative content of different oxygen species on the catalyst surface was obtained. The results in the sequence of  $\alpha/\beta/\gamma$  are as follows: 4/86/10 (P3), 8/78/14 (P7) and 14/74/12 (P9), Accordingly, with the pH decrease in the synthesis process by the addition of HAc, the percentage of O<sup>-</sup> species was improved, but with pH increase in the synthetic process by addition of KOH, the percentage of O<sup>-</sup> species was reduced, so sample P3 has the highest O-content, and P9 has the lowest. In addition, O<sup>2-</sup> and O<sup>-</sup> species are known as chemical absorption of surface active oxygen species, many studies have demonstrated that O<sup>2-</sup> and O<sup>-</sup>

species were the activity oxygen species in the catalytic oxidation reaction. It is directly related to the oxygen cavity of catalyst. The total content of O<sup>2-</sup> and O<sup>-</sup> in the sample increases in the sequence of P3 > P7 > P9, this also suggests that the pH changing in the Pt loading process will directly affect the amount of oxygen cavity. The lower the pH in the preparation is, the more oxygen cavities in the catalyst are. Oxygen cavities can not only adsorb oxygen, but also can activate oxygen, then to keep recycling of the surface active oxygen, thus improve the catalyst activity in the NO auxiliary atmosphere.

## 2.6 NO + O<sub>2</sub> in situ DRIFTS

In order to study NO<sub>x</sub> storage way, in situ DRIFTS was carried out on sample P3, P7, P9, the reaction atmosphere is 400×10<sup>-6</sup> NO + 10% O<sub>2</sub> + N<sub>2</sub>. The adsorption results are shown in Fig.8~10.

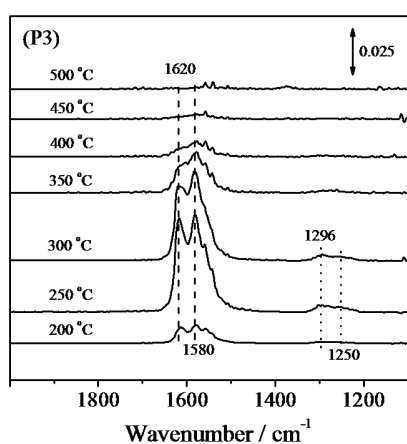


Fig.8 In-Situ DRIFTS on catalysts P3 at different temperatures

图 8 P3 催化剂在不同温度下的原位傅立叶红外图

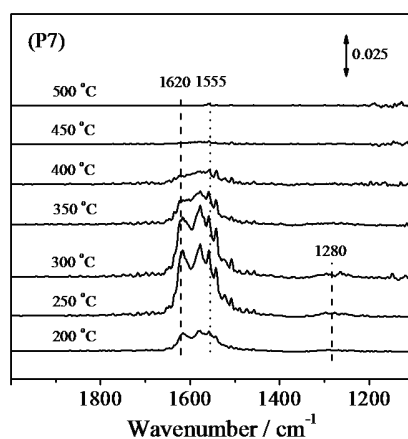


Fig. 9 In-Situ DRIFTS on catalysts P7 at different temperatures

图 9 P7 催化剂在不同温度下的原位傅立叶红外图

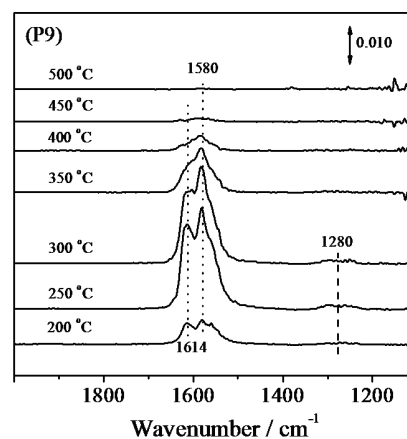


Fig.10 In-Situ DRIFTS on catalysts P9 at different temperature

图 10 P9 催化剂在不同温度下的原位傅立叶红外图

It could be observed that the NO<sub>x</sub> adsorption behaviors of the catalyst could be divided into two stages, in the first stage (200~300 °C), the peak positions in 1250 and 1296 cm<sup>-1</sup> can be attributable to single tooth nitrates<sup>[25]</sup>, and the peak position in 1580 cm<sup>-1</sup> can be attributable to bidentate nitrate, the peak at 1620 cm<sup>-1</sup> is NO<sub>2</sub> absorption peak<sup>[26-28]</sup>. It is worth mentioned that infrared intensity of the above species reached maximum at 250 °C, means strongest adsorp-

tion. In the second stage (300~500 °C), the peak of the single tooth nitrate is eliminated (1250 cm<sup>-1</sup> and 1296 cm<sup>-1</sup>), and the peak intensities of bidentate nitrate and NO<sub>2</sub> absorption are gradually weakened, finally disappeared at around 500 °C. The adsorption behavior of sample P7 was similar with sample P3, the peak at 1620 cm<sup>-1</sup> is corresponding bidentate nitrates<sup>[26]</sup>. The difference between P3 and P9 is that NO<sub>2</sub> absorption peak of P9 shifts from 1620 cm<sup>-1</sup> to 1615 cm<sup>-1</sup> [27-28]. In

addition, the intensity of infrared absorption peak in the sample increases in the sequence of P3 > P7 > P9, this is consistent with the active order.

According to the results of infrared analysis, it can be concluded that bidentate nitrate and NO<sub>2</sub> absorption peaks that formed on the catalyst surface are the reactive nitrogen oxygen species, the stronger the peak intensity of both, the better the soot elimination performance in the NO + O<sub>2</sub> atmosphere.

### 2.7 Sulfur and water resistance performance of the catalyst

The soot elimination performance in NO atmosphere for the samples that pretreated in different concentrations of water and sulfur is shown in Fig. 11.

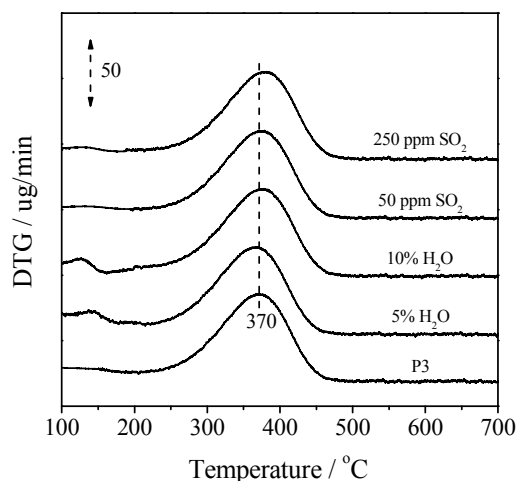


Fig. 11 DTG curves for different catalysts

(The reaction atmosphere is  $400 \times 10^{-6}$  NO + 10% O<sub>2</sub> + N<sub>2</sub>).

图 11 不同催化剂的 DTG 曲线

(反应气氛  $400 \times 10^{-6}$  NO + 10% O<sub>2</sub> + N<sub>2</sub>)

As seen from Fig. 11, the samples that treated in different concentrations of water and sulfur have the same soot elimination performance with the untreated P3 catalyst under NO atmosphere. The  $T_m$  difference among the catalysts is less than 8°C, so it could be considered the five catalysts have the same activity. The Pt catalyst that made of CeO<sub>2</sub>-TiO<sub>2</sub>-Al<sub>2</sub>O<sub>3</sub> support with good thermal stability has excellent resistance to water and sulfur.

### 3 Conclusion

A series of catalysts Pt/CeO<sub>2</sub>-TiO<sub>2</sub>-Al<sub>2</sub>O<sub>3</sub> were prepared by impregnation method, through changing

the pH of Pt loading process, the soot elimination performance under NO atmosphere was studied carefully. The results showed that the lower pH of Pt loading process, the catalysts possess greater Pt particle size, larger amount of chemisorbed surface active oxygen species (O<sub>2</sub><sup>-</sup>, O<sup>-</sup>) and better soot elimination performance. Moreover, according to the results of *in-situ* DRIFT, it is concluded that bidentate nitrates and adsorbed NO<sub>2</sub> are the active intermediate species. Different concentrations of H<sub>2</sub>O and SO<sub>2</sub> resistant test were carried out on the P3 catalyst, it is found that the performance changed little before and after poisoning, which implies that the stability of catalyst is good and has an industrial application prospect.

### References:

- [1] Brown D M, Wilson M R, MacNee W, et al. Size dependent Proinflammatory effects of ultrafine polystyrene particles a role for surface area and oxidative stress in the enhanced activity of ultrafines[J]. Toxicol Appl Pharm [J], 2001, 175(3): 191-199.
- [2] Fino D, Cauda E, Mescia D, et al. LiCoO<sub>2</sub> catalyst for diesel particulate abatement[J]. Catal Today, 2007, 119(1): 257-261.
- [3] Olong N E, Stöwe K, Maier W F, A combinatorial approach for the discovery of low temperature soot oxidation catalysts[J]. Appl Catal B, 2007, 74(1/2): 19-25.
- [4] Fino D, Russo N, Saracco G, et al. Catalytic removal of NO<sub>x</sub> and diesel soot over nanostructured spinel-type oxides[J]. J Catal, 2006, 242(1): 38-47.
- [5] Allansson R, Cooper B J, Thoss J E, et al. European experience of high mileage durability of continuously regenerating diesel particulate filter technology[R]. SAE Technical Paper, 2000.
- [6] Yoshida K, Makino S, Sumiya S, et al. Simultaneous reduction of NO<sub>x</sub> and particulate emissions from diesel engine exhaust[R]. SAE Technical Paper, 1989.
- [7] Cooper B J, Thoss J E. Role of NO in diesel particulate emission control[R]. SAE Technical Paper, 1989.
- [8] Bueno-López A, Krishna K, Makkee M et al. Enhanced soot oxidation by lattice oxygen via La<sup>3+</sup>-doped CeO<sub>2</sub>[J]. J Catal, 2005, 230(1): 237-248.
- [9] Escobar J, De los Reyes J A, Viveros T, Influence of the synthesis additive on the textural and structural

- characteristics of sol-gel Al<sub>2</sub>O<sub>3</sub>-TiO<sub>2</sub>[J]. *Ind Eng Chem Res*, 2000, 39(3): 666-672.
- [10] Matsumoto S, Ikeda Y, Suzuki H et al. NO<sub>x</sub> storage-reduction catalyst for automotive exhaust with improved tolerance against sulfur poisoning[J]. *Appl Catal B*, 2000, 25(2-3): 115-124.
- [11] Atribak I, Bueno-López A, García-García A. Uncatalysed and catalysed soot combustion under NO<sub>x</sub>+ O<sub>2</sub>: real diesel versus model soots[J]. *Combust Flame*, 2010, 157(1): 2086-2094.
- [12] Wei Y C, Liu J, Zhao Z, et al. The catalysts of three-dimensionally ordered macroporous Ce<sub>1-x</sub>Zr<sub>x</sub>O<sub>2</sub> supported gold nanoparticles for soot combustion: The metal-support interaction[J]. *J Catal*, 2012, 287(1): 13-29.
- [13] Sing K S W, Everett D H, Haul R A W, et al. Reporting physisorption data for gas/solid systems with special reference to the determination of surface area and porosity [J]. *Pure Appl Chem*, 1985, 57(4): 603-619.
- [14] Avila M S, Vignatti C I, Apesteguía C R, et al. Effect of V<sub>2</sub>O<sub>5</sub> loading on propane combustion over Pt/V<sub>2</sub>O<sub>5</sub>-Al<sub>2</sub>O<sub>3</sub> catalysts[J]. *Catal Lett*, 2010, 134(1-2): 118-123.
- [15] Liu S, Wu X D, Weng D, et al. NO<sub>x</sub>-Assisted soot oxidation on Pt-Mg/Al<sub>2</sub>O<sub>3</sub> catalysts: Magnesium precursor, Pt particle size, and Pt-Mg interaction[J]. *Ind Eng Chem Res*, 2012, 51(5): 2271-2279.
- [16] Maeda N, Urakawa A, Sharma R, et al. Influence of Baprecursor on structural and catalytic properties of Pt-Ba/alumina NO<sub>x</sub> storage-reduction catalyst[J]. *Appl Catal B*, 2011, 103(1/2): 154-162.
- [17] Schmitz P J, Kudla R J, Drews A R, et al. NO oxidation over supported Pt: Impact of precursor, support, loading, and processing conditions evaluated via high throughput experimentation[J]. *Appl Catal B*, 2006, 67(3/4): 246-256.
- [18] Mulla S S, Chen N, Cumarantunge L, et al. Reaction of NO and O<sub>2</sub> to NO<sub>2</sub> on Pt: Kinetics and catalyst deactivation[J]. *J Catal*, 2006, 241(2): 389-399.
- [19] Setiabudi A, Makkee M, Moulijn J A, The role of NO<sub>2</sub> and O<sub>2</sub> in the accelerated combustion of soot in diesel exhaust gases[J]. *Appl Catal B*, 2004, 50(3): 185-194.
- [20] Liotta L F, Catalytic oxidation of volatile organic compounds on supported noble metals[J]. *Appl Catal B*, 2010, 100(3/4): 403-412.
- [21] Li L D, Shen Q, Cheng J, et al. Catalytic oxidation of NO over TiO<sub>2</sub> supported platinum clusters I. Preparation, characterization and catalytic properties [J]. *Appl Catal B*, 2010, 93(3/4): 259-266.
- [22] Caballero A, Holgado J P, Gonzalez-delaCruz V M, et al. In situ spectroscopic detection of SMSI effect in a Ni/CeO<sub>2</sub> system: hydrogen-induced burial and dig out of metallic nickel[J]. *Chem Commun*, 2010, 46(3): 1097-1099.
- [23] Wei Y, Liu J, Zhao Z, et al. Highly active catalysts of gold nanoparticles supported on three-dimensionally ordered macroporous LaFeO<sub>3</sub> for soot oxidation[J]. *Angew Chem*, 2011, 123(10): 2374-2377.
- [24] Wei Y, Liu J, Zhao Z, et al. Three-dimensionally ordered macroporous Ce<sub>0.8</sub>Zr<sub>0.2</sub>O<sub>2</sub>-supported gold nanoparticles: Synthesis with controllable size and super-catalytic performance for soot oxidation[J]. *Energy Environ Sci*, 2011, 4(8): 2959-2970.
- [25] Lin F, Wu X D, Weng D, Effect of barium loading on CuO<sub>x</sub>-CeO<sub>2</sub> catalysts: NO<sub>x</sub> storage capacity, NO oxidation ability and soot oxidation activity[J]. *Catal Today*, 2011, 175(1): 124-132.
- [26] Wu X D, Liu S, Lin F, et al. Nitrate storage behavior of Ba/MnO<sub>x</sub>-CeO<sub>2</sub> catalyst and its activity for soot oxidation with heat transfer limitations[J]. *J Hazard Mater*, 2010, 181(1/3): 722-728.
- [27] Hadjiivanov K I, Identification of neutral and charged N<sub>x</sub>O<sub>y</sub> surface species by IR spectroscopy[J]. *Catal Rev*, 2000, 42(1/2): 71-144.
- [28] Liu J, Zhao Z, Chen Y S, et al. Different valent ions-doped cerium oxides and their catalytic performances for soot oxidation[J]. *Catal Today*, 2011, 175(1): 117-123.